



HAL
open science

Host Cell Geometry and Cytoskeletal Organization Governs Candida-Host Cell Interactions at the Nanoscale

Easter Ndlovu, Lucas Malpartida, Taranum Sultana, Tanya Dahms, Etienne
Dague

► **To cite this version:**

Easter Ndlovu, Lucas Malpartida, Taranum Sultana, Tanya Dahms, Etienne Dague. Host Cell Geometry and Cytoskeletal Organization Governs Candida-Host Cell Interactions at the Nanoscale. ACS Applied Materials & Interfaces, 2023, 15 (44), pp.50789-50798. 10.1021/acsami.3c09870 . hal-04244012

HAL Id: hal-04244012

<https://laas.hal.science/hal-04244012>

Submitted on 16 Oct 2023

HAL is a multi-disciplinary open access archive for the deposit and dissemination of scientific research documents, whether they are published or not. The documents may come from teaching and research institutions in France or abroad, or from public or private research centers.

L'archive ouverte pluridisciplinaire **HAL**, est destinée au dépôt et à la diffusion de documents scientifiques de niveau recherche, publiés ou non, émanant des établissements d'enseignement et de recherche français ou étrangers, des laboratoires publics ou privés.



Distributed under a Creative Commons Attribution - NoDerivatives 4.0 International License

This document is confidential and is proprietary to the American Chemical Society and its authors. Do not copy or disclose without written permission. If you have received this item in error, notify the sender and delete all copies.

Host Cell Geometry and Cytoskeletal Organization Governs Candida-Host Cell Interactions at the Nanoscale

Journal:	<i>ACS Applied Materials & Interfaces</i>
Manuscript ID	am-2023-098705.R3
Manuscript Type:	Article
Date Submitted by the Author:	06-Oct-2023
Complete List of Authors:	Ndlovu, Easter; University of Regina, Chemistry and Biochemistry Malpartida, Lucas; Laboratoire d'analyse et d'architecture des systemes, NanoBioSystem Sultana, Taranum; University of Regina, Chemistry and Biochemistry Dahms, Tanya; University of Regina, Chemistry and Biochemistry Dague, Etienne; Laboratoire d'analyse et d'architecture des systemes, NanoBioSystem

SCHOLARONE™
Manuscripts

Host Cell Geometry and Cytoskeletal Organization Governs *Candida*-Host Cell Interactions at the Nanoscale

Easter Ndlovu¹, Lucas Malpartida², Taranum Sultana¹, Tanya E. S. Dahms^{*1}, Etienne Dague^{*2}

¹Department of Chemistry and Biochemistry University of Regina, 3737 Wascana Parkway, Regina, SK, S4S 0A2, Canada

²National Centre for Scientific Research, Laboratory for Analysis and Architecture of Systems (LAAS). 7 avenue du Colonel Roche, BP 54200, 31031, Toulouse, cedex 4, France

*Co-corresponding authors: tanya.dahms@uregina.ca (TESD), edague@laas.fr (ED)

ABSTRACT

Candida is one of the most common opportunistic fungal pathogens in humans. Its adhesion to the host cell is required in parasitic states, and is important for pathogenesis. Many studies have shown that there is an increased risk of developing candidiasis when normal tissue barriers are weakened or when immune defences are compromised for example during cancer treatment that induces immunosuppression. The mechanical properties of malignant cells, such as adhesiveness and viscoelasticity, which contribute to cellular invasion and migration are different from those of non-cancerous cells. To understand host invasion and its relationship with host cell health, we probed the interaction of *Candida* spp. with cancerous and non-cancerous human cell lines using atomic force microscopy in single cell force spectroscopy mode. There was significant adhesion between *Candida* and human cells, with more adhesion to cancerous versus non-cancerous cell lines. This increase in adhesion is related to the mechanobiological properties of cancer cells which have a disorganized cytoskeleton and lower rigidity. Altered geometry and cytoskeletal disruption of the human cells impacted adhesion parameters, underscoring the role of cytoskeletal organisation in *Candida*-human cell

1
2
3 adhesion and implicating the manipulation of cell properties as a potential future
4
5 therapeutic strategy.
6
7
8

9 **KEYWORDS:** Single-cell Force Spectroscopy, adhesion force, host-pathogen
10 interaction, cytoskeleton organisation, micro-contact patterning, cancerous vs non-
11 cancerous.
12
13
14
15
16
17
18
19
20
21
22
23
24
25
26
27
28
29
30
31
32
33
34
35
36
37
38
39
40
41
42
43
44
45
46
47
48
49
50
51
52
53
54
55
56
57
58
59
60

INTRODUCTION

Human opportunistic pathogens such as fungi play an important role in causing superficial mucosal and disseminated infections,^{1,2} including those of the oral cavity, gastrointestinal tract and vaginal surfaces,² for which systemic infections can lead to severe morbidity. *Candida* spp. are the most common pathogenic fungal microorganisms, and in particular *Candida albicans* is the leading cause of the fungal infection candidiasis worldwide.^{2,3} Although *C. albicans* is the most commonly isolated species, other non-*albicans* strains have emerged. For example, *Candida glabrata* is the second most frequently isolated *Candida* species reported as the causative agent of increased infection rates.^{1,3-5} Despite the shared genus, *C. albicans* and *C. glabrata* are quite distinct, suggesting that infection-causing interactions with their host may differ.⁶

To invade and infect host cells, *Candida* must first come in direct contact with host mucosal surfaces, the first line of defense against pathogen invasion of underlying tissues.^{5,7-9} *Candida* spp. have developed a number of commensal and virulence traits that enable it to adhere to and colonize host tissues during infection,¹⁰ including morphological changes,^{10,11} biofilm formation, secretion of hydrolytic enzymes and the expression of adhesins and invasins (host cell receptors).^{2,12-14}

One of *Candida*'s key pathogenicity virulence factors^{8,13,15} is its ability to adhere to a diverse set of surfaces, allowing it to colonize the host through multiple avenues.^{1,3,16} Surfaces can be either abiotic, for example intravascular and urinary catheters, prosthetic cardiac valves and denture prostheses, or biotic, including a variety of tissues within the human body, such as human skin keratinocytes, the subendothelial matrix and epithelial mucosal tissues,^{1,17,18} offering a variety of host niches.^{4,9} The adhesion of *Candida* to

1
2
3 epithelial cells is a multifactorial process defined by the close association between yeast
4 cell wall components and epithelial surface proteins.^{7,14,15,19}
5
6

7
8
9 Expression of these fungal and host surface proteins, along with other key factors such
10 as hydrolytic enzyme and toxin secretion, govern adhesion.^{7,16,19,20} Environmental factors
11 such as temperature, pH, medium type and the presence of carbohydrates (glucose,
12 sucrose),^{16,21} along with non-specific factors such as pathogen surface hydrophobicity
13 and electrostatic forces, can alter external protein content, impacting fungal-epithelial cell
14 adhesion.^{21–24} Further, epithelial cell morphology also plays a role in fungal-host cell
15 adhesion,²⁵ which is regulated by the cytoskeleton, comprised of microfilaments,
16 intermediate filaments, microtubules and actin filaments.²⁶
17
18
19
20
21
22
23
24
25
26

27
28 Initial yeast to epithelium contact may begin with non-specific contact, followed by
29 adhesion through physical forces (e.g. Waals interaction, hydrophobicity, electrostatic)²⁷
30 and finally specific host-cell interactions between lectin-like proteins on the yeast cell wall
31 and glycoproteins on the host cells.²⁷ Given the ever-increasing prevalence of *Candida*-
32 related infections, the events and mechanisms involved in the initial interactions between
33 *Candida* species (*glabrata* and *albicans*) and host epithelial cells were of interest. Using
34 atomic force microscopy (AFM) single cell force spectroscopy (SCFS) at pN-scale
35 resolution we measured intercellular interactions^{28–30} between *Candida* and cancerous
36 and non-cancerous human cell lines: skin keratinocytes (HaCaT), human gingival
37 fibroblasts (HGF), human vaginal epithelial (VK2/E6E7), human cervical epithelial cancer
38 (HeLa) and human epithelial colorectal adenocarcinoma (CaCo2). To examine the role of
39 the cytoskeleton, we assessed the influence of host cell shape (round, squares, Y) on
40 yeast adhesion. Our data provide insight into the strength of *Candida*-mammalian cell
41
42
43
44
45
46
47
48
49
50
51
52
53
54
55
56
57
58
59
60

1
2
3 interactions and the role of cellular mechanobiological properties such as cell shape and
4
5 cytoskeletal arrangement on these interactions, offering insight into new therapeutic
6
7 avenues for preventing and treating fungal-induced disease.
8
9

10 11 12 **RESULTS**

13 14 ***C. albicans* adhere strongly to human skin, vaginal and oral cell lines**

15
16 To study the interaction between yeast and its host at the nanoscale level, we first had to
17
18 establish that the effects were biological rather than nonspecific comparing the interaction
19
20 of *Candida* to that of a silica bead. To do so, we used SCFS with a tipless cantilever.
21
22 Probes were created using a 5 μm diameter silica bead attached to a tipless cantilevers
23
24 coated with a thin layer of UV-curable glue, while a concanavalin A coated cantilever was
25
26 used to immobilize a single *Candida*. Each probe was used to approach a human cell line
27
28 at a speed of 20 $\mu\text{m/s}$ and withdrawn at a constant speed. During the approach and
29
30 retraction of the probes towards the center of epithelial cells (Figure S1), force-distance
31
32 curves were recorded. While single silica microspheres had very low adhesion (Figure
33
34 1a), frequently below 20 pN, *C. albicans* comparatively had 5-fold higher adhesion to
35
36 HaCaT cells (Figure 1b, 1b inset). The maximum adhesion force between single live cells
37
38 of *Candida albicans* and HaCaT increased with contact time from 0 (101 pN) to 5 (321
39
40 pN) s, but not significantly at longer durations (Figure 1d). These interactions were also
41
42 expressed as work of adhesion, with more force requiring greater work to separate
43
44 adhering molecules (Figure 1e). Interestingly, maximum rupture length (43 μm) was not
45
46 impacted by contact time (Figure 1f). Analysis of the force retract curve (Figure 1c) shows
47
48 no interaction between the bead and the HaCaT cells, as expected (top curve), as
49
50 compared to unique binding events for the interaction between *C. albicans* and human
51
52
53
54
55
56
57
58
59
60

1
2
3 cell lines. Retraction curves, associated with long rupture distances, show jumps
4 resembling step-like unbinding events with a rise in the force before the unbinding of
5 single adhesive units, and long plateaus showing tethers associated with stretching of a
6 cell membrane tube before the adhesive units can unbind.^{31–33}
7
8
9

10
11 Having demonstrated that the adhesion of *C. albicans* to skin keratinocytes increases
12 with contact time, we next investigated its adhesion to other cell lines, since epithelial cell
13 type, morphology and differentiation stage have been reported to determine the strength
14 of adhesion.¹⁶ Interactions between the yeast and VK2/E6E7 vaginal cells were probed,
15 based on the frequency of vulvovaginal candidiasis,³⁴ and HGF cells, based on the link
16 between *Candida* and oral carcinoma.^{27,35,36} Figure 1g shows that binding of *C. albicans*
17 to HGF and VK2 results in similar adhesive strength and patterns. Similar to Figure 1a-d,
18 there was a very low binding force between these human cells and the bead, which was
19 significantly greater with *C. albicans*, with an increase from 0 to 5 s. Although HGF cells
20 had similar adhesion patterns to VK2 cells, the *C. albicans* adhesion force to VK2 was
21 higher (780.5 pN at 5s) than to HGF (528.6 pN at 5s) cells (Figure 1g). The adhesion
22 work (Figure 1h) and rupture length (Figure 1i) showed a similar trend to that of adhesion
23 force. It is interesting to note that there was no significant difference between the rupture
24 distances for HGF cells at all 4 contact times, but for VK2 cells between 0 s and 20 s the
25 rupture distance averaged 35 and 45 μm , respectively (Figure 1i).
26
27
28
29
30
31
32
33
34
35
36
37
38
39
40
41
42
43
44
45
46
47
48
49
50
51
52
53
54
55
56
57
58
59
60

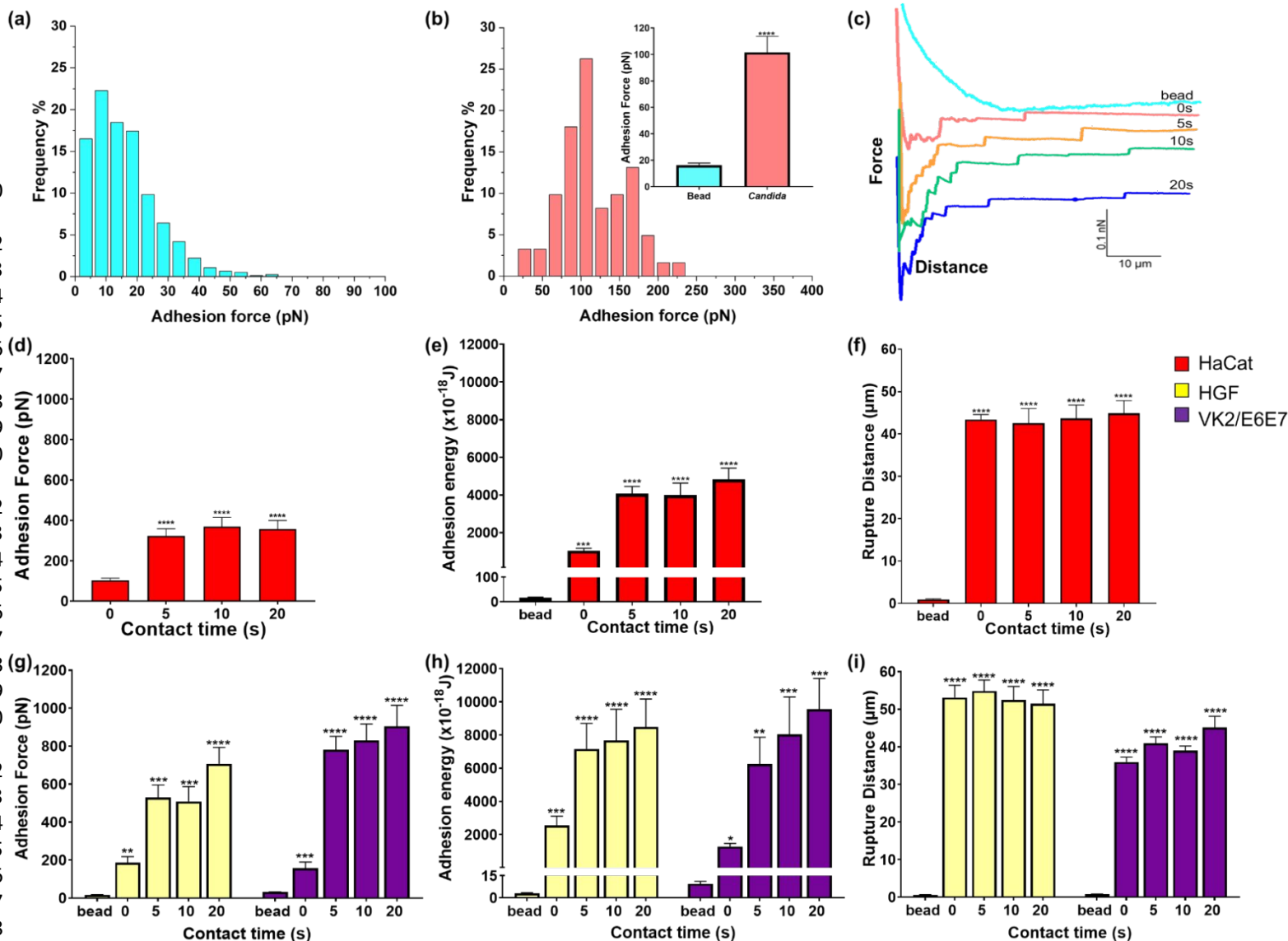


Figure 1. HaCaT, HGF and VK2/E6E7 cells show strong interactions with *C. albicans*. Histograms show percentage frequency adhesion between (a) beads and (b) *C. albicans* with the HaCaT cell line. Cell-cell interactions were quantified as (d, g) maximal adhesion force, (e, h) adhesion energy and (f, i) rupture lengths for HaCaT (c, e, f), HGF and VK2/E6E7 (g, h, i), as well as (c) typical force retraction curves for HaCaT (turquoise - bead, pink - 0s, orange - 5s, green - 10s and blue - 20s) showing rupture events for contact times of 0, 5, 10 and 20s. Results represent at least three (\pm SEM) independent experiments in which at least three human cells were probed with a different *C. albicans* for each contact time, generating 100 force curves each. An unpaired t-test and one-way ANOVA analysis of variance with Bonferroni post-tests were used to determine statistical differences (ns, $p > 0.05$; *, $p < 0.05$; **, $p < 0.01$; ***, $p < 0.001$; ****, $p < 0.0001$).

1
2
3 **Binding force of *C. glabrata* to human cells is similar to that of *C.***
4 ***albicans*.**
5
6
7

8 *C. glabrata* is the most frequently isolated non-*Candida albicans* (NCA) species and is
9 also the second most common cause of candidiasis.³⁻⁵ We therefore investigated the host
10 pathogen interactions between *C. glabrata* and the HaCaT, VK2 and HGF cell lines. Like
11 the *C. albicans*-HaCaT (Figure 1c) interaction, the *C. glabrata*-HaCaT interaction is also
12 strengthened with more contact time (Figure 2b) and shows a typical force curve, as
13 observed for *C. albicans* and mammalian cells, with multiple jumps and tethers (Figure
14 2a). It is noteworthy that *C. glabrata*-HaCaT had the lowest interaction force (348 pN)
15 compared to HGF (759 pN) and VK2 (927 pN) at 20 s. The adhesion energy was
16 proportional to the maximal adhesion force (Figure 2c), with no significant difference ($p >$
17 0.05) between the rupture distances at all contact times and all three cell lines (Figure
18 2d). Taken together, *C. glabrata* and *C. albicans* bind in a similar manner to human cell
19 lines.
20
21
22
23
24
25
26
27
28
29
30
31
32
33
34
35
36
37
38
39
40
41
42
43
44
45
46
47
48
49
50
51
52
53
54
55
56
57
58
59
60

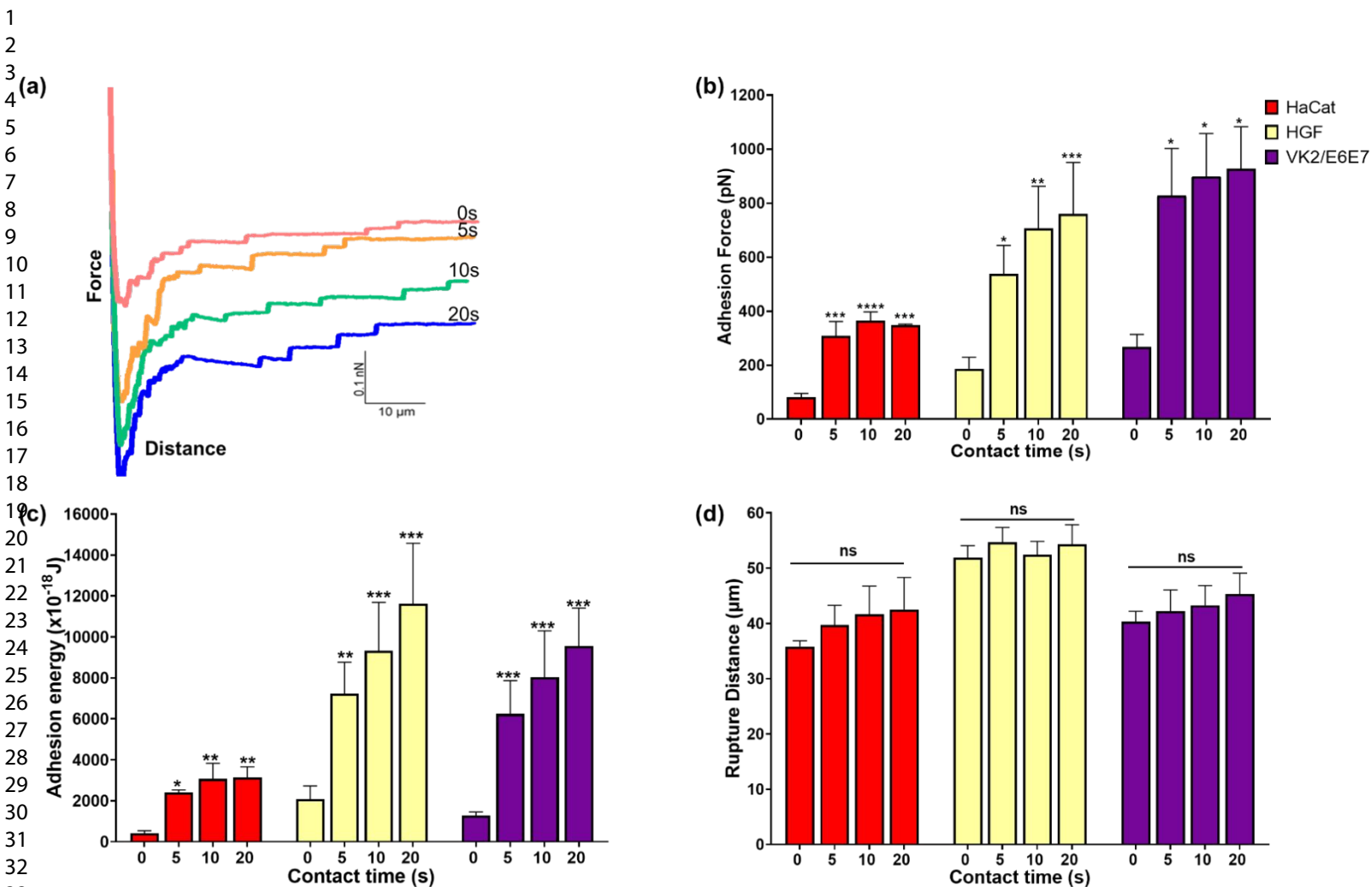
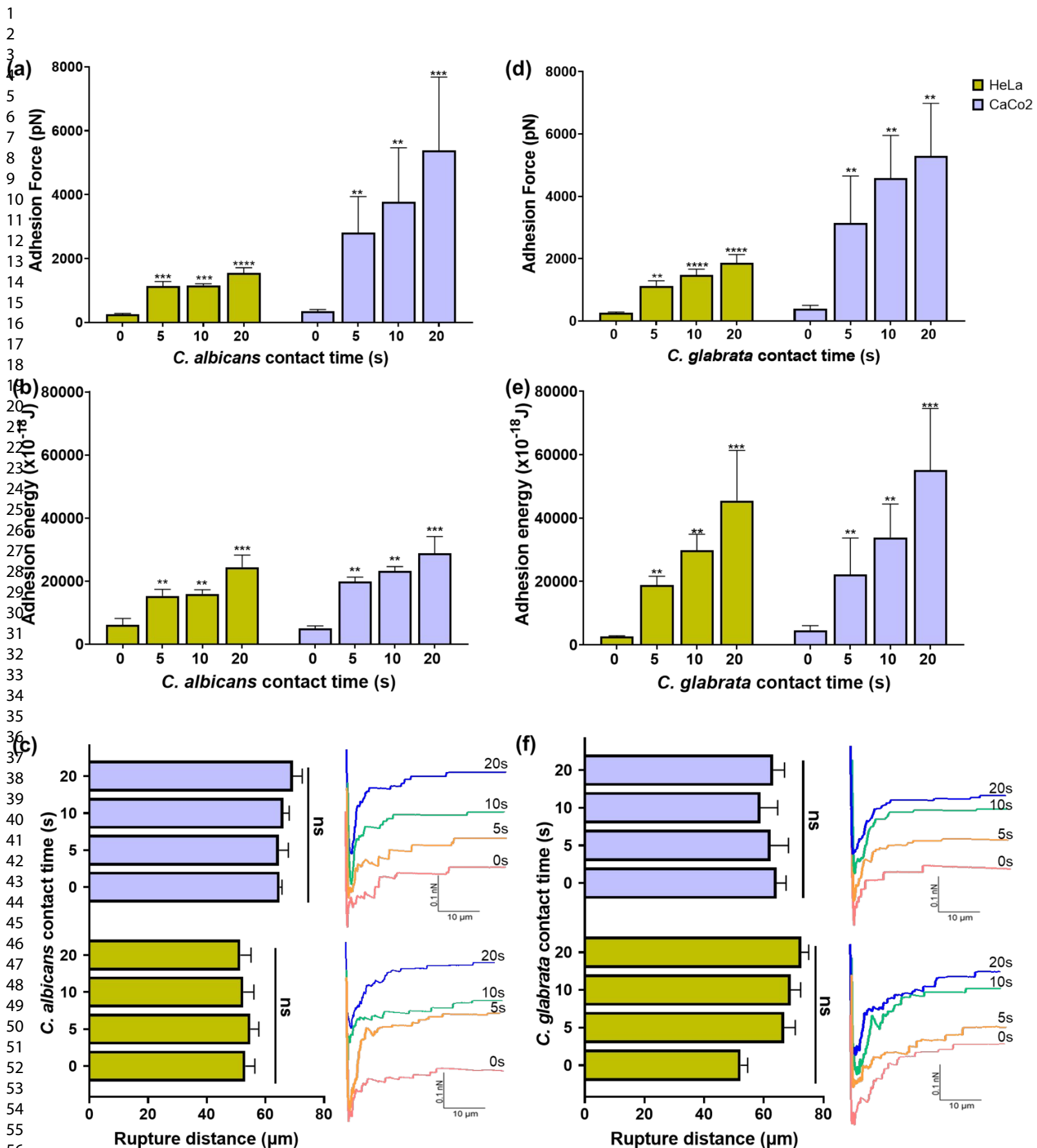


Figure 2. *C. glabrata* binds to mammalian cells in a similar manner to *C. albicans*. Cell-cell interactions are shown as the (a) retraction force distance curves for the interaction between *C. glabrata* and the HaCaT cell line (pink - 0s, orange - 5s, green - 10s and blue - 20s), (b) maximal adhesion force, (c) adhesion energy and (d) rupture distance between *C. glabrata* and HaCaT, HGF and VK2/E6E7 cells at contact times of 0, 5, 10 and 20s. Results are expressed as the mean \pm SEM for at least three biological replicates in which at least three human cells were probed with a different *C. glabrata* for each contact time, generating 100 force curves each. Statistical difference was calculated from a one-way ANOVA analysis of variance with Bonferroni post-tests (*, **, *** and **** represent, $p < 0.05$, $p < 0.01$, $p < 0.001$, and $p < 0.0001$, respectively).

***Candida* adheres more strongly to cancerous cells**

Having established biological adhesion between *Candida* and the mammalian cell lines, the adhesion between *Candida* and 2 human cancer cell lines was examined: CaCo2 (colon cancer) was chosen as the gut is a *Candida* reservoir^{37,38} and HeLa (cervical cancer) since *Candida* is responsible for more than 90% of cervicovaginal infections.^{39,40} HeLa and CaCo2 cell lines adhered to both *C. albicans* and *C. glabrata*, with a maximal adhesion force for *Candida*.

HeLa that increased with contact time (Figure 3a,d). Despite similar adhesion patterns, there were significant differences in maximal force, for example a more than 3-fold difference in adhesion at 5 s for *C. albicans*-HeLa (1136 pN, Figure 3a) as compared to *C. albicans*-HaCaT (321 pN, Figure 1c). Interestingly, there was a very strong adhesion force between CaCo2 cells and both *C. albicans* and *C. glabrata* (Figure 3a,d), two fold larger than that for HeLa cells. As expected, the adhesion energy (Figure 3b,e) was proportional to the adhesion force and there was no difference between rupture lengths (Figure 3c,f). Tether length could not be captured as it was limited by the z-range (100 μm) of the CellHesion AFM head. Overall, cancerous cells had distinct adhesion patterns, higher adhesion energy (Figure 3b,e) and longer rupture lengths (Figure 3c,f) for both yeast strains.



1
2
3 **Figure 3.** *Candida* strains adhere more strongly to cancer cell lines. Interactions shown as (a, d)
4 maximal adhesion force, (b, e) adhesion energy and (c, f) rupture length as well as (c, f) typical
5 force-distance curves (pink - 0s, orange - 5s, green -.10s and blue - 20s) for the interaction
6 between *C. albicans* and *C. glabrata* and HeLa and CaCo2 cell lines. Results are representative
7 of at least three (mean \pm SEM) independent biological replicates with 100 force curves recorded
8 at a contact time of 0, 5, 10 and 20s. One-way ANOVA analysis of variance with Bonferroni post-
9 tests (*, **, *** and **** represent, $p < 0.05$, $p < 0.01$, $p < 0.001$, and $p < 0.0001$, respectively) was
10 used to determine statistical differences.
11
12
13
14
15

16 17 **Adhesion of yeast strains to human cells is facilitated by host cell** 18 **cytoskeletal arrangement** 19

20 Cellular processes such as cell survival, growth and differentiation are affected by cell
21 shape and size, thus making cell geometry a vital regulator of cell physiology.⁴¹ Human
22 cells cultured on fibronectin micropatterned coverslips had pattern-driven geometries
23 (Figure S3a,b): circular, square and Y-shaped, all with a 20 x 20 μm^2 surface area. AFM
24 measurements clearly showed differences in shape-dependent adhesion forces between
25 the different cell morphologies (Figure 4a,b), with a 2-fold increase in adhesion force
26 between the Y-shaped HaCaT cells and both yeast strains (Figure 4a). The square
27 morphology had an approximately 1.5-fold and 2-fold increase in adhesion to *C. albicans*
28 and *C. glabrata*, respectively, whereas the circular morphology (Figure 4a) showed a
29 statistically significant increase in adhesion for *C. glabrata* but not *C. albicans*. There was
30 an almost identical result for the adhesion of *C. albicans* to the HaCaT and HeLa
31 (immortalized cancer) cell lines, with the square and Y-shaped morphologies having a
32 significant increase in adhesion, but no significant increase in adhesion between *C.*
33 *glabrata* and the circular-shaped HeLa cells (Figure 4b). Interestingly we did not observe
34 any changes in adhesion for VK2/E6E7 cells except for the Y-shaped probed with *C.*
35 *glabrata* (Figure S3c,d). Collectively, these results indicate that host cell shape plays a
36
37
38
39
40
41
42
43
44
45
46
47
48
49
50
51
52
53
54
55
56
57

significant role in adhesion in addition to contributions from different adhesion molecules associated with *C. albicans* and *C. glabrata*.

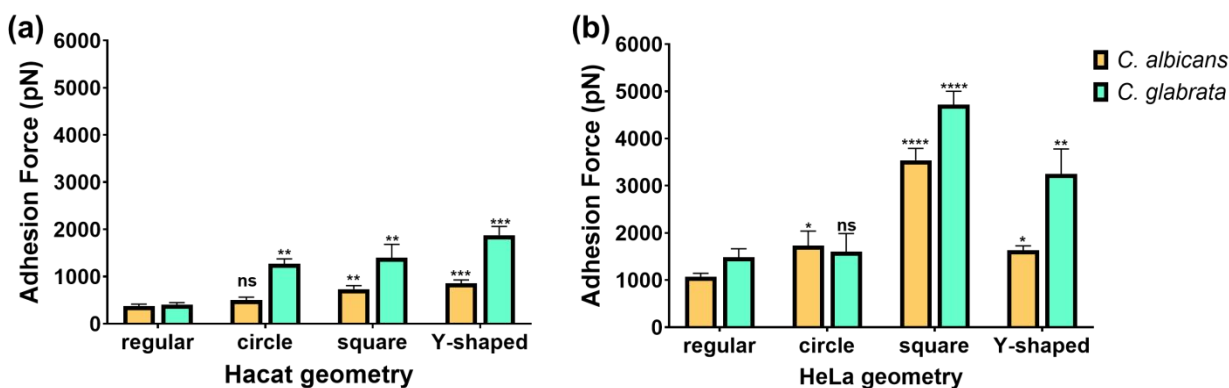
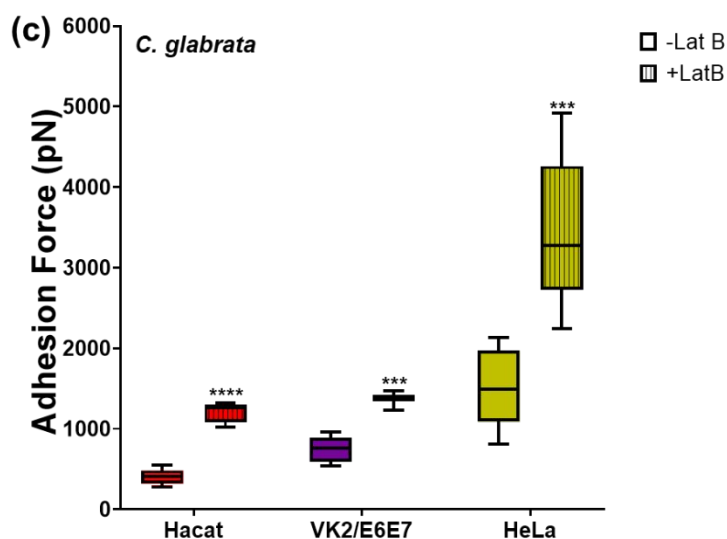
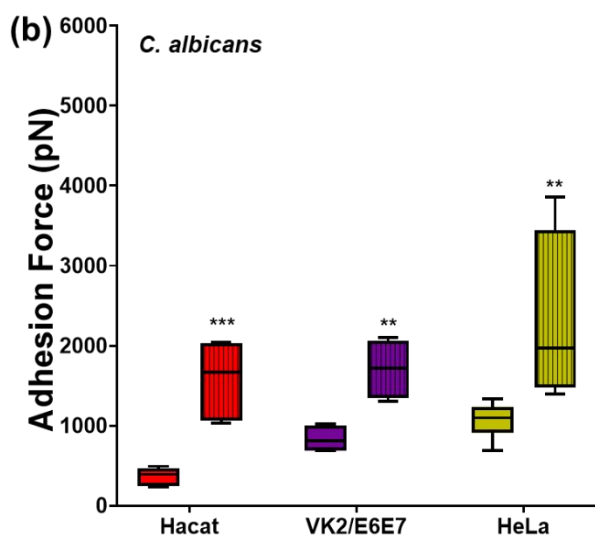
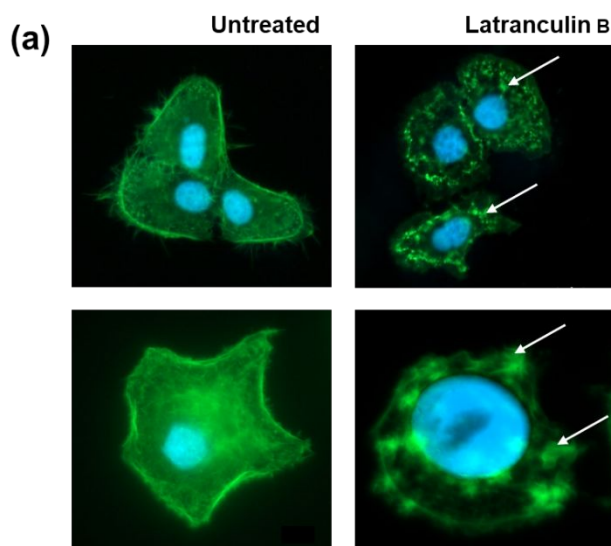


Figure 4. Human cell line geometry induces changes in *Candida* adhesion. Maximal adhesion measurements for normal, circular, square and Y-shaped live cells are shown for both yeast strains (*C. albicans* and *C. glabrata*) with (a) HaCaT and (b) HeLa cell lines micropatterned onto coverslips with fibronectin patterns. Results are expressed as the mean \pm SEM for at least three biological replicates having different yeast probes and at least 100 force curves per yeast strain. A one-way ANOVA analysis of variance with Bonferroni post-tests gave rise to no statistical significance, ns, or varying statistical significance; *, $p < 0.05$; **, $p < 0.01$; ***, $p < 0.001$; ****, $p < 0.0001$ between experiments.

Since a change in cell morphology is associated with cytoskeletal rearrangement,⁴¹ we examined the role of the cytoskeleton in cell-cell adhesion and cellular mechanical properties. Based on the known decrease in CHO cell elasticity when treated by Latrunculin B (LatB) (Louise et al. (2014)), we explored the impact of cytoskeletal depolymerization on yeast-human cell adhesion. Cells were treated with 0.1 μ M of LatB and incubated for 30 mins to achieve optimal depolymerization as determined by Louise et al.⁴² Epifluorescence microscopy confirmed LatB-induced cytoskeletal disruption,⁴² with actin dispersal and aggregation in LatB treated cells compared to the uniform actin

1
2
3 distribution of untreated cells (Figure 5a, S4). LatB-treated human cells probed with *C.*
4 *albicans* and *C. glabrata* by SCFS had an approximately 1.5-fold increased adhesion for
5 both the non-cancerous and cancer cell lines (Figure 5b,c). Taken together, this provides
6 substantial evidence that cytoskeleton arrangement plays a significant role in regulating
7 adhesion (Figure 4, 5).
8
9
10
11
12
13
14
15



1
2
3
4
5
6
7 **Figure 5.** Cytoskeletal depolymerization leads to an increase in cell-cell adhesion. (a)
8 Representative immunofluorescence images of HaCaT (non- cancerous) and HeLa (cancerous)
9 cells untreated or treated with LatB (white arrow show aggregation of F-actin) and stained with
10 DAPI (blue) and F-actin (green). Scale bars are 10 μm . (b-c) Box plots show the distribution of
11 adhesion values for depolymerized cells (HaCaT, VK2/E6E7 and HeLa) probed with (b) *C.*
12 *albicans* and (c) *C. glabrata*. Results shown are representative of at least three biological
13 replicates, having different yeast probes and at least 100 force curves analyzed per strain.
14 Asterisks *, $p < 0.05$; **, $p < 0.01$; ***, $p < 0.001$; ****, $p < 0.0001$ represent statistical significance
15 from an unpaired t-test.
16
17
18

19 DISCUSSION

20
21 One of the crucial virulence attributes of *Candida* is its ability to invade a number of
22 different tissues within the host, allowing it to occupy many host niches.^{9,25} This
23 opportunistic pathogen has developed strategies for adhesion, cellular invasion,
24 intracellular survival and proliferation.²⁵ To provide evidence for our hypothesis that
25 candidiasis occurs more frequently in cancer patients not only because of
26 immunosuppression, but also because of an intrinsic difference in adhesion between
27 *Candida* and the cancerous and non-cancerous cells, we aimed to quantify *Candida*-
28 mammalian cell interactions. The majority of *Candida*-human cell adhesion studies use
29 standard adhesion assays in which adherent cells are visualized using fluorescence
30 microscopy and quantified by counting the number of adherent yeasts.^{15,25,43} More
31 recently, SCFS has been used to quantify adhesion forces between single live yeast and
32 mammalian cells.⁴⁴
33
34
35
36
37
38
39
40
41
42
43
44
45
46
47

48 *C. albicans* adhesion to skin keratinocyte, gingival fibroblast and vaginal epithelial cell
49 lines was found to be implicitly biological (Figure 1), consistent with prior studies of other
50 pathogens, with similar adhesion profiles.^{45,46} The adhesion of *Candida* to human cells is
51 a multifactorial process defined by the close association between yeast cell wall
52
53
54
55
56
57

1
2
3 components and human cell surface macromolecules (reviewed in ⁷), necessitating time
4 for *Candida* to invade the host. Indeed, maximal adhesion between *C. albicans* and all
5 human cell lines increased with contact time (Figure 1), in agreement with⁴⁴ who report a
6 time-dependent increase in adhesion between *Candida* and macrophages. Increased
7 contact time allows for more receptors to engage in the interaction, and in the context of
8 immune cells allows the cell membrane more time to engulf the yeast with greater surface
9 area.^{47,48} The work of adhesion and the rupture lengths⁴⁴ in this study (Figures 1,2) agree
10 with interactions between microbe-mammalian cells,^{45,49} with the large adhesion energy
11 attributed to deformability of the host cell membrane.^{44,45} Jumps and tethers, as well as
12 long rupture length during yeast detachment would also increase the duration of contact
13 between the host and pathogen (Figure 1c, 2a, 3c,f).⁴⁴

14
15
16
17
18
19 In addition to *C. albicans*, other NCA species,^{50,51} such as *C. glabrata* are responsible for
20 mucosal and systemic infections.⁵² Previous studies report percent adhesion of *C.*
21 *glabrata* to various human cells,^{4,13} but not interaction forces. Like *C. albicans*, *C. glabrata*
22 adheres to the HaCaT, HGF and VK2 cells (Figure 2), consistent with the selective
23 adhesion of mammalian cells compared to cell culture plates.¹³ Adhesion force, work and
24 rupture length between *C. glabrata* and VK2 cells (Figure 2) are consistent with a prior
25 study.⁵³

26
27
28
29
30
31
32
33
34
35
36
37
38
39
40
41
42
43
44
45
46
47
48
49
50
51
52
53
54
55
56
57
58
59
60
C. albicans adhere more strongly to mammalian cells as compared to NCA species,^{16,54}
attributed to the greater number of α -L-fucose residues within cell surface
glycoconjugates.⁵⁴ Further, *C. albicans* adhere better to vascular endothelium than *C.*
glabrata, which may relate to the lack of adhesins on *C. glabrata*.⁵⁵ However, *C. glabrata*
is also known to encode a large repertoire of surface proteins, including the EPA family

1
2
3 of adhesins that are directly implicated in mammalian cell adhesion.^{1,3,4,17} It is worth
4
5 noting, that prior studies report percentage adhesion, which does not necessarily
6
7 translate to stronger adhesion forces, and so is not inconsistent with this study which
8
9 showed no clear differences between the two *Candida* strains (Figure S5).

10
11
12
13 While the high risk of immunocompromised individuals developing *Candida* infection is
14
15 well known,^{35,56,57} there is increasing evidence that *Candida* can produce carcinogenic
16
17 substances that play a role in cancer development,^{58,59} prompting us to probe *Candida*
18
19 interactions with immortalized cell lines from human cancer (Figure 3). *Candida* spp.
20
21 adhered to HeLa (cervical cancer) and CaCo2 (human colorectal adenocarcinoma) cells
22
23 with much greater force than non-cancerous cell lines. The completely different adhesion
24
25 ranges between cancerous and non-cancerous cells can be attributed to cell elasticity,⁸
26
27 with cancer cell lines having significantly lower Young's moduli compared to non-
28
29 cancerous ones (Figure S2). It is well known that non-cancerous cells are stiffer than
30
31 cancerous ones (cancer cells are softer), with the degree of cancerous cell elasticity
32
33 related to their histological origin,⁶⁰ for example cervical cancer cells have greater
34
35 elasticity than those from lung and breast tissue.⁶⁰ Thus, differences in cell elasticity
36
37 (Figure S2) may explain variable adhesion with different cancer cell lines, and indeed
38
39 softer cells are more easily deformed, leading to a larger probe-cell contact area thus
40
41 giving rise to higher adhesion.⁶¹

42
43
44
45
46
47
48
49 Since cancer cells have a disorganized cytoskeleton and generally lower rigidity, we
50
51 hypothesized that the surface area of the initial contact phase would be greater, along
52
53 with adhesion. Consistent with this idea, we found that reorganization of the cell
54
55 cytoskeleton, either by altering cell shape or chemical means, impacted *Candida*-human
56
57

1
2
3 cell adhesion (Figure 4 and 5). Shape-dependent stiffness has been correlated to cell
4
5 contractility⁴¹ and larger cells tend to have greater stiffness,⁶² further underscoring how
6
7 mechanical behaviour depends on cell type.
8
9

10
11 Cytoskeletal F-actin not only contributes to cell shape, but is the primary polymer system
12
13 responsible for regulating cell stiffness,⁶³ with cellular elasticity increasing as a function
14
15 of F-actin.⁶⁰ In this study, depolymerization of human cell F-actin filaments led to
16
17 increased adhesion with both *Candida* strains (Figure 5), irrespective of the cell line used.
18
19 Indeed, depolymerization of CHO cell actin with LatB not only decreases cell elasticity
20
21 over time but also impacts cell shape.⁴² Results showing higher adhesion in patterned
22
23 cells was corroborated by Young's moduli calculations showing differences in elasticity
24
25 when cells were patterned into different shapes (Figure S3e,f). When cells were patterned
26
27 into Y-shapes on a 20 x 20 μm^2 surface area they took the shape of a triangle (Figure
28
29 S3b), indeed a previous study has shown differences in elasticity between triangle,
30
31 square and circular human mesenchymal stem cells.⁴¹ F-actin regulates a number of
32
33 macromolecules involved in cell-cell adhesion, which explains the change in adhesion
34
35 with cytoskeletal rearrangement (Figures 4, 5). Our results showing the important role of
36
37 the cytoskeletal organization on the adhesion of microbes to host cells represents a major
38
39 discovery in the field. Interestingly, artificial epithelial cells made from soft silicone
40
41 substrates coated with E-cadherin adhesins, essential for cell-to-cell cohesion, mimic
42
43 epithelial cells and importantly illustrate how adhesin distribution is dependent on the
44
45 elasticity of the system.⁶⁴ Thus, it is likely that changes in cell elasticity can alter adhesin
46
47 distribution, which would ultimately affect cell adhesion as observed in this study. In fact,
48
49 actin cytoskeletal rearrangement, including filament assembly and polymerization,
50
51
52
53
54
55
56
57

1
2
3 contribute to *C. albicans* host invasion, thus contributing fatal candidemia.⁶⁵ Von Erlach
4
5 et al. (2018) hypothesized that based on the association of the cytoskeleton with the
6
7 human cell membrane, the cytoskeletal biophysical state regulates the activity of cell
8
9 signalling proteins associated with plasma membrane microdomains.⁴¹
10
11
12
13
14
15
16
17
18
19
20
21
22
23
24
25
26
27
28
29
30
31
32
33
34
35
36
37
38
39
40
41
42
43
44
45
46
47
48
49
50
51
52
53
54
55
56
57
58
59
60

CONCLUSION

In summary, in this study we used the AFM SCFS at the single cell level to quantify microbe-mammalian cell interactions, showing *C. albicans* and *C. glabrata* strongly adhere to epithelial cells, with almost six-fold stronger adhesion to cancer cell lines. It has always been assumed that cancer patients are more susceptible to candidiasis based on their weakened immune system, but our findings reveal that enhanced cell-to-cell adhesion could also play a significant role. Human cell mechanobiology properties such as cytoskeletal rearrangement, known to alter cell elasticity, led to increased yeast-host adhesion. This research provides detailed mechanistic information on an opportunistic fungal pathogen, and identifies manipulation of cellular adhesion factors as a new therapeutic target for *Candida* infections.

METHODS

Yeast strains and culture conditions

The *C. glabrata* KUE100₈₂ strain was a kind gift from Prof Miguel Teixeira, and *C. albicans* was obtained from ABC Platform® Bugs Bank (Nancy, France). Strains were stored at -80°C and then revived on Yeast extract Peptone Dextrose (YPD) agar plates (Difco) at 30°C under static conditions. Single colonies were then picked from the plates, inoculated into YPD growth medium (10 g/L yeast extract, 20 g/L peptone and 20 g/L glucose) (Difco) and grown overnight at 30°C in an orbital shaker at 180 rpm.

Mammalian cell culture

The human gingival fibroblast (HGF-1) cell line, human cervix epithelial cells (HeLa), human skin keratinocytes (HaCaT), human colon epithelial cells (CaCo2) and the human

1
2
3 vaginal epithelial cell line (VK2/E6E7) immortalized with E6 and E7 genes of the human
4
5 papilloma virus 16 (HPV-16) cell lines were used in this study. HGF-1, HeLa, HaCaT and
6
7 CaCo2 were purchased from ATCC (catalog numbers, CRL-2014, CCL-2, CRL-2404,
8
9 HTB-37 respectively), and VK2/E6E7 (ATCC CRL-2616) was obtained from Prof Miguel
10
11
12 Teixeira (Universidade de Lisboa Instituto Superior Tecnico, Portugal).
13

14
15 HGF-1, HeLa, HaCaT and CaCo2 cells were maintained in Dulbecco's Modified Eagle
16
17 Medium (DMEM) supplemented with 1% penicillin streptomycin (penstrep) (Gibco, Fisher
18
19 Scientific) and 10% or 20% (CaCo2 cells) fetal bovine serum (FBS). Briefly, cells were
20
21 maintained in 75 cm² flasks at a temperature of 37°C with 90% humidity and 5% CO₂,
22
23
24 passaged when a confluency of 70-80% was reached, detached from the flask using
25
26 trypsin and the reaction was neutralized using DMEM. Cell suspensions were centrifuged
27
28
29 at 200 x g for 4 min, the pellet resuspended in medium and the cells seeded into flasks
30
31
32 for growth as described above.
33

34
35 The VK2/E6E7 cell line was maintained in keratinocyte serum-free medium (KSFM)
36
37 supplemented with 0.1 ng/mL human recombinant epidermal growth factor (EGF), 44.1
38
39 mg/L calcium chloride (CaCl₂) and 0.05 mg/mL bovine pituitary extract (BPE) (Gibco,
40
41 Fisher Scientific). Cells were cultured in 25 cm² flasks, at a temperature of 37°C with 90%
42
43 humidity, 5% CO₂, and passaged when a confluency of approximately 80% was reached.
44
45
46 Cells were detached by incubating with trypsin for 4 min, neutralized by the addition of 3
47
48 ml of a 1:1 nutrient mixture of DMEM (Gibco, Fisher Scientific) and Ham's F-12
49
50 supplemented with 10% FBS (HyClone, Fisher Scientific), centrifuged at 100 × g for 5
51
52
53 min, followed by resuspension in KSFM in flasks.
54
55

Single cell force spectroscopy

Single cell force spectroscopy (SCFS) was used to study the interaction between yeast and human cells. Firstly, NPO10 (Bruker, USA) triangular shaped AFM tipless cantilevers (Bruker, USA) were functionalized using the lectin Concanavalin A (conA; Sigma Aldrich). Cantilevers were cleaned for 2 min using oxygen plasma at a pressure of 0.4 mbar, then immersed in 100 $\mu\text{g/mL}$ of conA solution overnight, and washed in acetate buffer (18 mM, pH 5.2) before use. AFM cell probes were then prepared by depositing an overnight culture of yeast cells into a petri dish and then the yeast picked up by the conA-coated cantilevers (Figure S1c) using the AFM (Nanowizard III AFM, Bruker, JPK). As a control, a 5 μm diameter silica bead (Bangs Laboratories) was attached to NPO10 cantilevers coated with a thin layer of UV-curable glue (NOA 63, Norland Edmund Optics) using the AFM. Single human-*Candida* cell interactions were measured using the AFM CellHesion[®] module under human cell growth conditions in a heated (Bruker, JPK BIOAFM) petri dish connected to a CO₂ tube and grown overnight (6×10^4 cells). The spring constant of the cantilevers was calibrated using the thermal noise method, having a sensitivity of approximately 18 to 35 nm/V and a spring constant (0.017 to 0.044 N/m), consistent with the nominal spring constant (0.06 N/m; Bruker, USA). The probes were then used to measure interaction forces within a 3 $\mu\text{m} \times 3 \mu\text{m}$ area at the center of the cell (Figure S1a,b) using an applied force of 0.5 nN with 20 $\mu\text{m/s}$ approach and retract speeds and contact times of 0 (immediate retraction), 5, 10 and 20 s. Each force curve was analyzed using the JPK Data Processing software (JPK, Berlin, Germany), for which adhesion force, work of adhesion and rupture distance histograms were calculated. Each condition

1
2
3 was evaluated with a minimum of three biological replicates and 5 cells for each replicate.
4
5 Yeast probes were replaced between technical repeats.
6
7

8 **Micropatterned substrates**

9
10 Microcontact printing was used to study the effect of cell shape on adhesion and
11
12 micropatterned substrates produced according to a method described by.⁶⁶ Briefly, poly-
13
14 dimethyl siloxane (PDMS) stamps were structured into different shapes (squares, circles,
15
16 and letter Y) of different sizes ranging from 10 to 60 μm using a silicon master mold which
17
18 was fabricated by photolithography as described by Foncy et al. (2018). The structured
19
20 PDMS stamp was then cleaned with an isopropanol rinse, dried with nitrogen gas and
21
22 then inked using 80 μl of 100 $\mu\text{g}/\text{ml}$ fibronectin (Sigma Aldrich) followed by a 3 min
23
24 incubation. Immediately before microcontact printing, a 2.2 \times 2.2 cm coverslip was
25
26 cleaned using oxygen plasma (Diener Pico) at a pressure of 0.6 mBar and 100% oxygen
27
28 for 1.5 s and was then brought into contact with the inked stamp for 3 min. The stamp
29
30 was removed, and to passivate the non-patterned area, 80 μl of 100 $\mu\text{g}/\text{ml}$ poly-L-lysine-
31
32 grafted-poly ethylene glycol (PLL-g-PEG) was added to the coverslip and incubated for
33
34 30 min, followed by aspiration of the PLL-g-PEG. The cover slip was then washed 3 times
35
36 with phosphate buffered saline (PBS), placed in a petri dish and stored in PBS at 4 $^{\circ}\text{C}$.
37
38 Human cells (5×10^4 cells per cm^2) were seeded onto the coverslip, incubated for 2 h to
39
40 allow attachment, the growth medium changed, and the cells further incubated for 4 h to
41
42 allow spreading into the pattern for SCFS.
43
44
45
46
47
48
49
50

51 **Latrunculin treatment**

52
53 To study the effect of actin cytoskeletal rearrangement on cell-cell adhesion, cells were
54
55 treated with latrunculin B (LatB; Tebu-bio), known to inhibit actin polymerization.⁶⁷
56
57

1
2
3 Following protocols described by Louise et al. (2014), cells (6×10^4) were seeded in a
4 petri dish and left overnight, then 0.1 μM of LatB in DMSO added to the cells, incubated
5
6 for 30 min, the medium aspirated, followed by two washes with 1ml PBS. The drug free
7
8 cell culture medium was used for probing cells by SCFS.
9
10

11 12 13 **Epifluorescence microscopy**

14
15 Fluorescence imaging was used to confirm the impact of LatB treatment. Cells were
16
17 cultured, confluent cells passaged, grown on clean 22×22 mm coverslips in DMEM
18
19 overnight, and treated with LatB as described above. Treated and control cells were
20
21 rinsed three times with 0.01 M PBS, permeabilized with 0.2% Triton X100 for 3 min,
22
23 washed again 3 times with 0.01 M PBS and then stained with 100 $\mu\text{g/ml}$ DAPI (Life
24
25 technologies) and 1X Phalloidin-iFluor 488 (Abcam) for 20 min, followed by 3 rinses with
26
27 0.01 M PBS. Coverslips were mounted on microscope slides using antifade mounting
28
29 media (Invitrogen), sealed using nail polish and imaged on a Zeiss Axio Observer Z1
30
31 inverted epifluorescence microscope (Zeiss, Oberkochen, Germany; DAPI - $\lambda_{\text{ex}} = 358$, λ_{em}
32
33 = 461; Phalloidine - $\lambda_{\text{ex}} = 495$, $\lambda_{\text{em}} = 518$).
34
35
36
37
38
39

40 41 **Statistical analysis**

42
43 GraphPad Prism® Software (version 9.2.0) was used for data manipulation, graphical
44
45 representations and statistical analyses. Unpaired t-tests were used to compare results
46
47 from two data sets and one-way ANOVA analysis of variance with a Bonferroni's post-
48
49 test, to compare all test data to control. Statistically significant differences of $p < 0.05$ (*),
50
51 $p < 0.01$ (**), $p < 0.001$ (***) or $p < 0.0001$ (****) are indicated in figures, and the absence
52
53 of an asterisk indicates no statistical difference, ($p > 0.05$, ns). Data are means from at
54
55 least biological replicates and error bars represent standard error of the mean (\pm SEM).
56
57

ASSOCIATED CONTENT

Supporting Information

AFM images of human cells in QI mode and yeast probe; Cell elasticity measurements of human cells probed with the bead; *Candida* adhesion to different human cell geometries; Cytoskeletal F-actin depolymerization following latrunculin b treatment; Comparison of *C. albicans* and *C. glabrata* adhesion to mammalian cells

AUTHOR INFORMATION

Corresponding Authors

Tanya Elizabeth Susan Dahms - Department of Chemistry and Biochemistry, University of Regina, 3737 Wascana Parkway, Regina, SK, S4S 0A2, Canada; orcid.org/0000-0002-8378-7480; Email: tanya.dahms@uregina.ca

Etienne Dague – LAAS-CNRS, Université de Toulouse, 7 Avenue du Colonel Roche, 31031 Toulouse, cedex 4, France; orcid.org/0000-0003-3290-9166; Email: edague@laas.fr

Authors

Easter Ndlovu - Department of Chemistry and Biochemistry, University of Regina, 3737 Wascana Parkway, Regina, SK, S4S 0A2, Canada

Lucas Malpartida - LAAS-CNRS, Université de Toulouse, 7 Avenue du Colonel Roche, 31031 Toulouse, cedex 4, France

Taranum Sultana - Department of Chemistry and Biochemistry, University of Regina, 3737 Wascana Parkway, Regina, SK, S4S 0A2, Canada

Author contributions

EN carried out the experimental work and data analysis, LM fabricated the PDMS patterns and generated micropatterns on the glass substrates. TS collected fluorescence images, EN, TESD and ED contributed to the hypotheses, experimental design, helped guide data analysis, interpretation, helped write and edit the manuscript.

Notes

The authors declare no competing interests.

ACKNOWLEDGMENTS

The work was supported by a Mitacs Globalink travel grant (Ref. IT12948) to EN, a Natural Science and Engineering Research Council Discovery Grant (NSERC DG; 06649-2018) to TESD, and Agence Nationale de la Recherche grant (Project-ANR-17-CE11-0023) to ED. EN was partially supported by the Faculty of Graduate Studies and Research at the University of Regina, which is situated on the traditional territories of the nêhiyawak, Anihsinapek, Nakoda, Dakota, and Lakota peoples, and the homeland of the Métis/Michif Nation.

We would like to thank the technical team at “caractérisation plateforme” at LAAS-CNRS especially, Charline Blatché, Sandrine Souleille and Camille Gironde for their training and guidance, Emmanuelle Trévisiol (Biosoft joint lab, LAAS-CNRS) for assistance generating the micropatterned substrates and Miguel Cacho Teixeira who provided the *C. glabrata* strain and the VK2/E6E7 cell line.

REFERENCES

- (1) de Groot PWJ, Bader O, de Boer AD, Weig M, Chauhan N. Adhesins in Human Fungal Pathogens: Glue with plenty of stick. *Eukaryot. Cell* **2013**, 12, 470–481.
- (2) Moyes DL, Richardson JP, Naglik JR. *Candida Albicans*-Epithelial Interactions and Pathogenicity Mechanisms: Scratching the Surface. *Virulence* **2015**, 6, 338–346.
- (3) Timmermans B, Peñas AD Las, Castaño I, Van Dijck P. Adhesins in *Candida Glabrata*. *J. Fungi* **2018**, 4, No. 60.
- (4) Cormack BP, Ghorri N, Falkow S. An Adhesin of the Yeast Pathogen *Candida Glabrata* Mediating Adherence to Human Epithelial Cells. *Science* **1999**, 285, 578-582.
- (5) Vale-Silva L, Ischer F, Leibundgut-Landmann S, Sanglard D. Gain-of-Function Mutations in PDR1, a Regulator of Antifungal Drug Resistance in *Candida Glabrata*, Control Adherence to Host Cells. *Infect. Immun.* **2013**, 81, 1709–1720.
- (6) Desai C, Mavrianos J, Chauhan N. *Candida Glabrata* Pwp7p and Aed1p are Required for Adherence to Human Endothelial Cells. *FEMS Yeast Res.* **2011**, 11, 595–601.
- (7) Richardson JP, Ho J, Naglik JR. *Candida*–Epithelial Interactions. *J. Fungi* **2018**, 4, No. 22.
- (8) Miyauchi M, Giummelly P, Yazawa S, Okawa Y. Adhesion of *Candida Albicans* to HeLa Cells: Studies using Polystyrene Beads. *Biol. Pharm. Bull.* **2007**, 30, 588-590.
- (9) Sohn K, Senyürek I, Fertey J, Königsdorfer A, Joffroy C, Hauser N, Zelt G, Brunner H, Rupp S. An in Vitro Assay to Study the Transcriptional Response During Adherence of *Candida Albicans* to Different Human Epithelia. *FEMS Yeast Res.* **2006**, 6, 1085–1093.
- (10) Höfs S, Mogavero S, Hube B. Interaction of *Candida Albicans* with Host Cells: Virulence Factors, Host Defense, Escape Strategies, and the Microbiota. *J. Microbiol.* **2016**, 54, 149–169.
- (11) Polke M, Hube B, Jacobsen ID. *Candida* Survival Strategies. *Adv. Appl. Microbiol.* **2015**, 91, 139-235.
- (12) Chaffin WL. *Candida Albicans* Cell Wall Proteins. *Microbiol. Mol. Biol. Rev.* **2008**, 72, 495–544.
- (13) Ichikawa T, Kutsumi Y, Sadanaga J, Ishikawa M, Sugita D, Ikeda R. Adherence and Cytotoxicity of *Candida* spp. To HaCaT and A549 cells. *Med. Mycol. J.* **2019**, 60, 5–10.
- (14) Gow NAR, Latge J-P, Munro CA. The Fungal Cell Wall: Structure, Biosynthesis, and Function. *Microbiol. Spectr.* **2017**, 5, 10–1128.
- (15) de Souza CM, Perini HF, Caloni C, Furlaneto-Maia L, Furlaneto MC. Adhesion of *Candida Tropicalis* to Polystyrene and Epithelial Cell Lines: Insights of Correlation of the Extent of Adherent Yeast Cells Among Distinct Surfaces. *J. Mycol. Med.* **2020**, 30, No. 101043.
- (16) Modrzewska B, Kurnatowski P. Adherence of *Candida* sp. to Host Tissues and Cells as one of its Pathogenicity Features. *Ann. Parasitol.* **2015**, 61, 3–9.
- (17) Valotteau C, Prystopiuk V, Cormack BP, Dufrêne YF. Atomic Force Microscopy Demonstrates that *Candida Glabrata* uses three Epa proteins to mediate

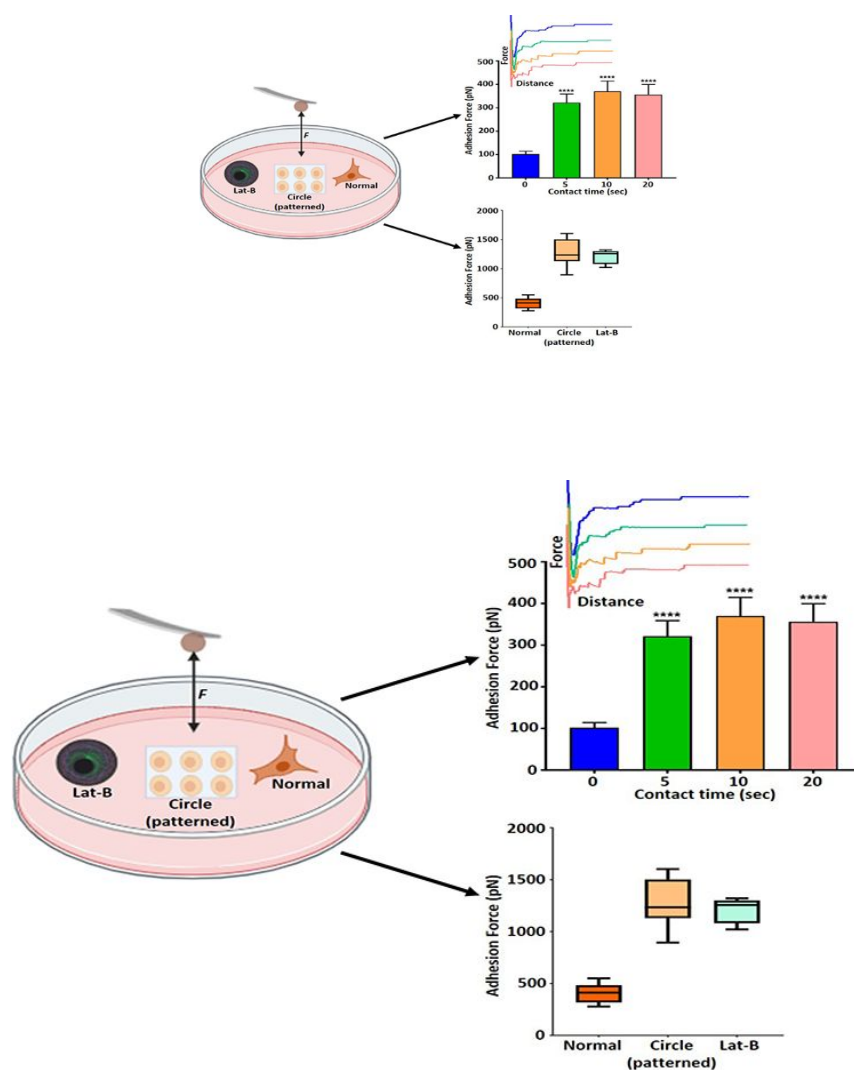
- 1
2
3
4
5
6
7
8
9
10
11
12
13
14
15
16
17
18
19
20
21
22
23
24
25
26
27
28
29
30
31
32
33
34
35
36
37
38
39
40
41
42
43
44
45
46
47
48
49
50
51
52
53
54
55
56
57
58
59
60
- adhesion to abiotic surfaces. *mSphere* **2019**, 4, 10-1128.
- (18) Lopez CM, Wallich R, Riesbeck K, Skerka C, Zipfel PF. *Candida Albicans* uses the Surface Protein Gpm1 to Attach to Human Endothelial Cells and to Keratinocytes via the Adhesive Protein Vitronectin. *PLoS One* **2014**, 9, No. 90796.
- (19) Hoyer LL. The ALS Gene Family of *Candida Albicans*. *Trends Microbiol.* **2001**, 9, 176–180.
- (20) Moyes DL, Wilson D, Richardson JP, Mogavero S, Tang SX, Wernecke J, Höfs S, Gratacap RL, Robbins J, Runglall M, Murciano C, Blagojevic M, Thavaraj S, Förster TM, Hebecker B, Kasper L, Vizcay G, Iancu SI, Kichik N, Häder A, Kurzai O, Luo T, Krüger T, Kniemeyer O, Cota E, Bader O, Wheeler RT, Gutschmann T, Hube B, Julian R, Naglik JR. Candidalysin is a Fungal Peptide Toxin Critical for Mucosal Infection. *Nature* **2016**, 532, 64–68.
- (21) Henriques M, Azeredo J, Oliveira R. *Candida* Species Adhesion to Oral Epithelium: Factors Involved and Experimental Methodology Used. *Crit. Rev. Microbiol.* **2006**, 32, 217–226.
- (22) Hazen KC. Participation of Yeast Cell Surface Hydrophobicity in Adherence of *Candida Albicans* to Human Epithelial Cells. *Infect. Immun.* **1989**, 57, 1894–1900.
- (23) Martin R, Wächtler B, Schaller M, Wilson D, Hube B. Host-Pathogen Interactions and Virulence-Associated Genes during *Candida Albicans* Oral Infections. *Int. J. Med. Microbiol.* **2011**, 301, 417–422.
- (24) Hazen KC, Lay JG, Hazen BW, Fu RC, Murthy S. Partial Biochemical Characterization of Cell Surface Hydrophobicity and Hydrophilicity of *Candida Albicans*. *Infect. Immun.* **1990**, 58, 3469–3476.
- (25) Dalle F, Wächtler B, L'Ollivier C, Holland G, Bannert N, Wilson D, Labruere C, Bonnin A, Hube B. Cellular Interactions of *Candida Albicans* with Human Oral Epithelial Cells and Enterocytes. *Cell Microbiol.* **2010**, 12, 248–271.
- (26) Scaife RM, Langdon WY. c-Cbl Localizes to Actin Lamellae and Regulates Lamellipodia Formation and Cell Morphology. *J. Cell Sci.* **2000**, 113, 215–226.
- (27) Sanjaya PR, Gokul S, Gururaj Patil B, Raju R. *Candida* in Oral Pre-Cancer and Oral Cancer. *Med. Hypotheses* **2011**, 77, 1125–1128.
- (28) Tejada-Mora H, Stevens L, Gröllers M, Katan A, van de Steeg E, van der Heiden M. AFM Based Elasticity of Intestinal Epithelium Correlate with Barrier Function under Drug Action. *bioRxiv* **2019**, No. 761627.
- (29) Dague E, Jauvert E, Laplatine L, Viallet B, Thibault C, Ressler L. Assembly of Live Micro-Organisms on Microstructured PDMS Stamps by Convective/Capillary Deposition for AFM Bio-Experiments. *Nanotechnology* **2011**, 22, No. 395102.
- (30) Bowen WR, Lovitt RW, Wright CJ. Atomic Force Microscopy Study of the Adhesion of *Saccharomyces Cerevisiae*. *J. Colloid Interface Sci.* **2001**, 237, 54–61.
- (31) Sariisik E, Popov C, Müller JP, Docheva D, Clausen-Schaumann H, Benoit M. Decoding Cytoskeleton-Anchored and Non-Anchored Receptors from Single-Cell Adhesion Force Data. *Biophys. J.* **2015**, 109, 1330–1333.
- (32) Lamers E, te Riet J, Domanski M, Luttge R, Figdor CG, Gardeniers JGE, Walboomers XF, Jansen JA. Dynamic cell adhesion and Migration on Nanoscale Grooved Substrates. *Eur. Cell Mater.* **2012**, 23, 182–194.

- 1
2
3 (33) Aguayo S, Bozec L. Mechanics of Bacterial Cells and Initial Surface Colonisation. *Adv. Exp. Med. Biol.* **2016**, 915, 245–260.
- 4
5 (34) Willems HME, Ahmed SS, Liu J, Xu Z, Peters BM. Vulvovaginal Candidiasis: A
6 Current Understanding and Burning Questions. *J. Fungi* **2020**, 6, No. 27.
- 7
8 (35) Alnuaimi AD, Wiesenfeld D, O'Brien-Simpson NM, Reynolds EC, McCullough MJ.
9 Oral *Candida* Colonization in Oral Cancer Patients and its Relationship with
10 Traditional Risk Factors of Oral Cancer: A Matched Case-Control Study. *Oral*
11 *Oncol.* **2015**, 51, 139–145.
- 12
13 (36) Bakri MM, Hussaini HM, Holmes A, Cannon RD, Rich AM. Revisiting the
14 Association Between Candidal Infection and Carcinoma, Particularly Oral
15 Squamous Cell Carcinoma. *J. Oral Microbiol.* **2010**, 2, No. 5780.
- 16
17 (37) Miranda LN, van der Heijden IM, Costa SF, Sousa AP, Sienna RA, Gobara S,
18 Santos CR, Lobo RD, Pessoa VP Jr Levin AS. *Candida* Colonisation as a Source
19 for Candidaemia. *J. Hosp. Infect.* **2009**, 72, 9–16.
- 20
21 (38) Nucci M, Anaissie E. Revisiting the Source of Candidemia: Skin or Gut? *Clin.*
22 *Infect. Dis.* **2001**, 33, 1959–1967.
- 23
24 (39) Godoy-Vitorino F, Romaguera J, Zhao C, Vargas-Robles D, Ortiz-Morales G,
25 Vázquez-Sánchez F, Vázquez-Sánchez M, de la Garza-Casillas M, Martinez-
26 Ferrer M, White JR, Bittinger K, Dominguez MG, Blaser MJ. Cervicovaginal Fungi
27 and Bacteria Associated with Cervical Intraepithelial Neoplasia and High-Risk
28 Human Papillomavirus Infections in a Hispanic Population. *Front. Microbiol.* **2018**,
29 9, No. 2533.
- 30
31 (40) Moradi S, Tadrís Hasani M, Darvish L, Roozbeh N. Evaluating Cervicovaginal
32 Infections and Cervical Cancer in Women with Low Socioeconomic Levels. *Iran J.*
33 *Public Health* **2017**, 46, 867–878.
- 34
35 (41) Von Erlach TC, Bertazzo S, Wozniak MA, Horejs CM, Maynard SA, Attwood S,
36 Robinson BK, Autefage H, Kallepitis C, Hernandez ADR, Chen CS, Goldini S,
37 Stevens MM. Cell-Geometry-Dependent Changes in Plasma Membrane order
38 Direct Stem Cell Signalling and Fate. *Nat. Mater.* **2018**, 17, 237–242.
- 39
40 (42) Louise C, Etienne D, Marie-Pierre R. AFM Sensing Cortical Actin Cytoskeleton
41 Destabilization during Plasma Membrane Electroporation. *Cytoskeleton*
42 **2014**, 71, 587–594.
- 43
44 (43) Biasoli MS, Tosello ME, Magaró HM. Adherence of *Candida* Strains Isolated from
45 the Human Gastrointestinal Tract. *Mycoses* **2002**, 45, 465–469.
- 46
47 (44) El-Kirat-Chatel S, Dufrêne YF. Nanoscale Adhesion Forces Between the Fungal
48 Pathogen: *Candida Albicans* and Macrophages. *Nanoscale Horizons* **2016**, 1, 69–
49 74.
- 50
51 (45) Prystopiuk V, Feuillie C, Herman-Bausier P, Viela F, Alsteens D, Pietrocola G,
52 Speziale P, Dufrêne YF. Mechanical Forces Guiding *Staphylococcus aureus*
53 Cellular Invasion. *ACS Nano* **2018**, 12, 3609–3622.
- 54
55 (46) Zuttion F, Ligeour C, Vidal O, Wälte M, Morvan F, Vidal S, Vasseur JJ, Chevolut
56 Y, Phaner-Goutorbe M, Schillers H. The Anti-Adhesive effect of Glycoclusters on:
57 *Pseudomonas Aeruginosa* Bacteria Adhesion to Epithelial Cells Studied by AFM
58 Single Cell Force Spectroscopy. *Nanoscale* **2018**, 10, 12771–12778.
- 59
60 (47) Helenius J, Heisenberg CP, Gaub HE, Muller DJ. Single-Cell Force Spectroscopy.
J. Cell Sci. **2008**, 121, 1785–1791.

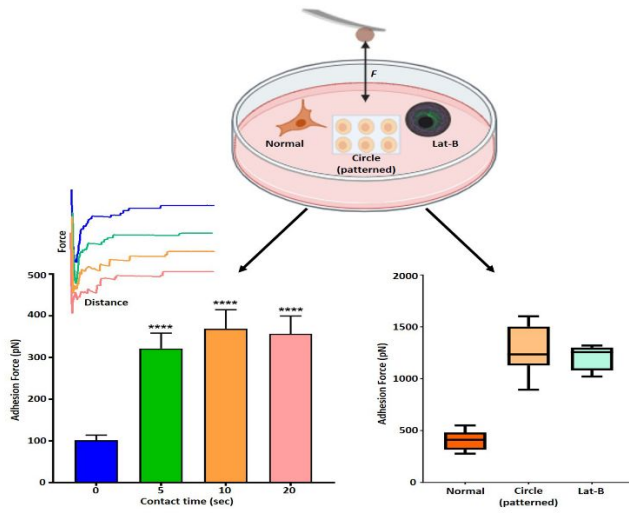
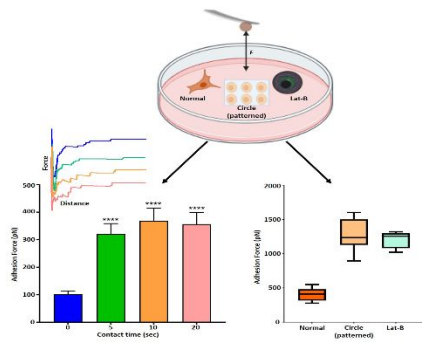
- 1
2
3 (48) Friedrichs J, Helenius J, Muller DJ. Quantifying Cellular Adhesion to Extracellular
4 Matrix Components by Single-Cell Force Spectroscopy. *Nat. Protoc.* **2010**, 5,
5 1353–1361.
6
7 (49) te Riet J, Joosten B, Reinieren-Beeren I, Figdor CG, Cambi A. N-glycan Mediated
8 Adhesion Strengthening during Pathogen-Receptor Binding Revealed by Cell-Cell
9 Force Spectroscopy. *Sci. Rep.* **2017**, 7, No. 6713.
10
11 (50) Nieminen MT, Uittamo J, Salaspuro M, Rautemaa R. Acetaldehyde Production
12 from Ethanol and Glucose by Non-*Candida Albicans* Yeasts in Vitro. *Oral Oncol.*
13 **2009**, 45, 245–248.
14
15 (51) Mäkinen A, Nawaz A, Mäkitie A, Meurman JH. Role of Non-*Albicans Candida* and
16 *Candida Albicans* in Oral Squamous Cell Cancer Patients. *J. Oral Maxillofac.*
17 *Surg.* **2018**, 76. 2564–2571.
18
19 (52) Antinori S, Milazzo L, Sollima S, Galli M, Corbellino M. Candidemia and Invasive
20 Candidiasis in Adults: A narrative review. *Eur. J. Intern. Med.* **2016**, 34, 21–28.
21
22 (53) Cavalheiro M, Pereira D, Formosa-Dague C, Leitão C, Pais P, Ndlovu E, Viana R,
23 Pimenta AI, Santos R, Takahashi-Nakaguchi A, Okamoto M, Ola M, Chibana H,
24 Fialho AM, Butler G, Dague E, Teixeira MC. From the First Touch to Biofilm
25 Establishment by the Human Pathogen *Candida Glabrata*: a Genome-Wide to
26 Nanoscale View. *Commun. Biol.* **2021**, 4, No. 886.
27
28 (54) Lima-Neto RG, Beltrão EIC, Oliveira PC, Neves RP. Adherence of *Candida*
29 *Albicans* and *Candida Parapsilosis* to Epithelial Cells Correlates with Fungal Cell
30 Surface Carbohydrates. *Mycoses* **2011**, 54, 23–29.
31
32 (55) Fidel PL, Vazquez JA, Sobel JD. *Candida glabrata*: Review of Epidemiology,
33 Pathogenesis, and Clinical Disease with Comparison to *C. Albicans*. *Clin.*
34 *Microbiol. Rev.* **1999**, 12, 80–96.
35
36 (56) Lekka M, Gil D, Pogoda K, Dulińska-Litewka J, Jach R, Gostek J, Klymenko O,
37 Prauzner-Bechcicki S, Stachura Z, Wiltowska-Zuber J, Okon K, Laidler P. Cancer
38 Cell Detection in Tissue Sections using AFM. *Arch. Biochem. Biophys.* **2012**, 518,
39 151–156.
40
41 (57) Chung LM, Liang JA, Lin CL, Sun LM, Kao CH. Cancer Risk in Patients with
42 Candidiasis: A Nationwide Population-Based Cohort Study. *Oncotarget* **2017**, 8,
43 63562–63573.
44
45 (58) Alnuaimi AD, Ramdzan AN, Wiesenfeld D, O'Brien-Simpson NM, Kolev SD,
46 Reynolds EC, McCullough MJ. *Candida* Virulence and Ethanol-Derived
47 Acetaldehyde Production in Oral Cancer and Non-Cancer Subjects. *Oral Dis.*
48 **2016**, 22, 805–814.
49
50 (59) Vadovics M, Jemima H, Igaz N, Alfodi R, Rakk D, Veres E, Szucs B, Horvath M,
51 Toth R, Szucs A, Csibi A, Horvath P, Tiszlavics L, Vagvolgyi C, Nosanchuk JD,
52 Szekeres A, Kiricsi M, Henley-smith R, Moyes DL, Thavaraj S, Brown R, Puskas
53 LG, Naglik JR, Gacser A. *Candida Albicans* Enhances the Progression of Oral
54 Squamous Cell carcinoma *In Vitro* and *In Vivo*. *Am. Soc. Microbiol.* **2022**, 13, No.
55 314421.
56
57 (60) Kwon S, Yang W, Moon D, Kim KS. Comparison of Cancer Cell Elasticity by Cell
58 Type. *J. Cancer* **2020**, 11, 5403–5412.
59
60 (61) Smolyakov G, Thiebot B, Campillo C, Labdi S, Severac C, Pelta J, Dague E.
Elasticity, Adhesion, and Tether Extrusion on Breast Cancer Cells Provide a

- 1
2
3 Signature of Their Invasive Potential. *ACS Appl. Mater. Interfaces* **2016**, *8*,
4 27426–27431.
- 5 (62) Nehls S, Nöding H, Karsch S, Ries F, Janshoff A. Stiffness of MDCK II Cells
6 Depends on Confluency and Cell Size. *Biophys. J.* **2019**, *116*, 2204–2211.
- 7 (63) Jalilian I, Heu C, Cheng H, Freittag H, Desouza M, Stehn JR, Bryce NS, Whan
8 RM, Hardeman EC, Fath T, Schevzov G, Gunning PW. Cell Elasticity is
9 Regulated by the Tropomyosin Isoform Composition of the Actin Cytoskeleton.
10 *PLoS One* **2015**, *10*, No. 126214.
- 11 (64) Eftekharijoo M, Chatterji S, Maruthamuthu V. Epithelial Cell-like Elasticity
12 Modulates E-cadherin Adhesion Organization. *ACS Biomater. Sci. Eng.* **2022**, *8*,
13 2455-2462.
- 14 (65) Yang W, Yan L, Wu C, Zhao X, Tang J. Fungal Invasion of Epithelial Cells.
15 *Microbiol. Res.* **2014**, *169*, 803–810.
- 16 (66) Foncy J, Estève A, Degache A, Colin C, Dollat X, Cau JC, Vieu C, Trevisiol E,
17 Malaquin L. Dynamic Inking of Large-Scale Stamps for Multiplexed Microcontact
18 Printing and Fabrication of Cell Microarrays. *PLoS One* **2018**, *13*, No. 202531.
- 19 (67) Rosazza C, Escoffre JM, Zumbusch A, Rols MP. The Actin Cytoskeleton has an
20 Active Role in the Electrotransfer of Plasmid DNA in Mammalian Cells. *Mol. Ther.*
21 **2011**, *19*, 913–921.
22
23
24
25
26
27
28
29
30
31
32
33
34
35
36
37
38
39
40
41
42
43
44
45
46
47
48
49
50
51
52
53
54
55
56
57
58
59
60

TABLE OF CONTENTS (TOC) graphic



1
2
3
4
5
6
7
8
9
10
11
12
13
14
15
16
17
18
19
20
21
22
23
24
25
26
27
28
29
30
31
32
33
34
35
36
37
38
39
40
41
42
43
44
45
46
47
48
49
50
51
52
53
54
55
56
57
58
59
60



1
2
3
4
5
6
7
8
9
10
11
12
13
14
15
16
17
18
19
20
21
22
23
24
25
26
27
28
29
30
31
32
33
34
35
36
37
38
39
40
41
42
43
44
45
46
47
48
49
50
51
52
53
54
55
56
57
58
59
60